Theoretical analysis of a recent experiment on mesoscopic state superpositions in cavity QED

F. Abbate, A. Messina,* and A. Napoli
INFM, MIUR and Dipartimento di Scienze Fisiche ed Astronomiche, Università di Palermo, via Archirafi 36, 90123 Palermo, Italy

F. Petruccione
School of Pure and Applied Physics, University of KwaZulu-Natal Durban, 4041, Durban, South Africa and Istituto Italiano per gli Studi Filosofici, Via Monte di Dio 14, I-80132 Napoli, Italy
(Received 8 March 2005; published 11 July 2005)

Quite recently quantum features exhibited by a mesoscopic field interacting with a single Rydberg atom in a microwave cavity has been observed [A. Auffeves *et al.*, Phys. Rev. Lett. **91**, 230405 (2003)]. In this paper we theoretically analyze all the phases of this articulated experiment considering from the very beginning cavity losses. Fully applying the theory of quantum open systems, our modelization succeeds in predicting fine aspects of the measured quantity, reaching qualitative and quantitative good agreement with the experimental results. This fact validates our theoretical approach based on the fundamental atom-cavity interaction model and simple mathematical structure of dissipative superoperators.

DOI: 10.1103/PhysRevA.72.013808 PACS number(s): 42.50.Dv, 03.65.Yz

I. INTRODUCTION

One of the principal problems arisen with the early development of quantum mechanics is that the linearity of the Schrödinger equation allows for the existence of superposition of macroscopically distinguishable states. Such states are never observed in common experience, which induces the question of the real existence of these states.

A series of recent experiments performed with atoms trapped in Paul-type traps [1–3] and with superconducting microwave cavities [4,5] have shown that "Schrödinger cat" states can indeed be created and observed. These experiments are typically performed in an intermediate mesoscopic domain between the microscopic and the macroscopic ones. Some experiments have clearly shown decoherence of the superposition of states due to the interaction of the system with the environment [6].

An important aspect of the experimental detection of nonclassical states is the adoption of an appropriate procedure to "probe" the system. Since the experiment is performed on a mesoscopic system the measurement act will necessarily alter its state. It is therefore necessary to describe the dynamics of the system by including the probing subsystem. Anyway it is evident that, whatever probing procedure is adopted, the exact relation between the effectively measured quantities and the state of the system itself must be clear.

Recently, a very interesting experiment [7] has shown that a Schrödinger cat state can be prepared and detected inside a superconducting microwave cavity. The state of the field inside the cavity is measured through a homodyne detection procedure, in which the field is indirectly measured by means of a probing atom. In this experiment, the quantity effectively measured is the probability $S_g(\phi)$ to find the probing atom in its ground state. This probability is obtained by varying the phase ϕ of the homodyne signal coupled to the cavity field.

In this paper we analyze from a theoretical point of view the results of this experiment. The interest in such an investigation stems from the possibility of exactly treating the dynamics of the system including from the very beginning and as much as possible the influence of the environment. The original paper reporting the experiment contains many physical ingredients to understand the qualitative behavior of the atom-field dynamics through the analysis of the measured probability $S_g(\phi)$ of finding the second atom in its ground state. We have, however, been stimulated by the fact that some aspects of the ϕ dependence of such a probability remain apparently unnoticed or at least not explained. What we are talking about is, for example, the presence of secondary maxima and minima in the $S_g(\phi)$ diffraction line pattern. The main contribution of this paper consists in an articulated and flexible theoretical platform which, including dissipative effects and assuming a Jaynes Cummings (JC) atom-field interaction model, provides an exact prediction of $S_g(\phi)$ which satisfactorily meets the experimental results.

The paper is structured as follows. In Sec. II we give a theoretical description of the experiment formulating in particular the Markovian quantum master equations ruling the dynamics of the system. The detailed analytical solution of the different phases of the time evolution of the system is presented in Sec. III and the subsequent one is devoted to the discussion of the probing procedure. The experiment is deeply analyzed in Sec. V and our conclusions are drawn in the last Sec. VI.

II. A THEORETICAL DESCRIPTION OF THE EXPERIMENT

In this section we give a short description of the experiment performed by Auffeves *et al.* [7] using the experimental setup sketched in Fig. 1.

The cavity used for the experiment is an open Fabry-Perot resonator made of two superconducting spherical niobium mirrors facing each other. The cavity has a quality factor Q

*Email address: messina@fisica.unipa.it

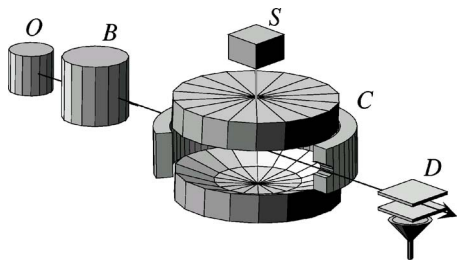

FIG. 1. Experimental apparatus.

$\simeq 10^8$ and sustains a Gaussian TEM_{900} mode at a frequency of 51.1 GHz with a $w=6-$mm waist.

Velocity selected ^{85}Rb atoms coming from the oven O are prepared, in zone B, in circular Rydberg states with principal quantum number $n=50$ and $n=51$. These atoms cross one by one the cavity C almost in perfect resonance with the transition between the two levels $n=50$ and $n=51$ hereafter denoted by $|g\rangle$ and $|e\rangle$, respectively.

Figure 2 aims at giving an idea of the three timing phases of the experiment. In phase 1 an atom A_1, initially prepared in $|e\rangle$ or $|g\rangle$, is injected into the cavity C. Just before the atom A_1 enters the cavity, a microwave signal F_1 prepares the resonator in a coherent state. The atom A_1 interacts with the cavity for a time T_1.

Phase 2 begins as soon as A_1 exits the cavity. A new microwave signal F_2, having the same amplitude of F_1 and relative phase $\phi+\pi$, is then injected inside the cavity. The phase ϕ is chosen in the interval between 0 and 2π and the experiment is performed many times with different values of ϕ.

In phase 3 a second atom, A_2, prepared in the $|g\rangle$ level crosses the cavity with the same speed of the first atom. Then, immediately after A_2 exits the resonator, its internal state is detected in D by means of static electric fields.

During phase 1 of the experiment the interaction between the atom and the cavity causes a splitting of the initial coherent state into two distinct coherent components locked with the two different atomic states [7]. The duration of the interaction T_1 is chosen such that the two coherent components are clearly separated. Such a separation is at the origin of a complete damping of the Rabi oscillations of the atom. Phase 1 leaves the cavity in a typical Schrödinger cat state. Of course dissipation sources tend to destroy the quantum coherence of this state within a time interval strictly related to the quality factor of the cavity.

Phases 2 and 3 of the experiment are designed so that they constitute an homodyne detection measurement.

To achieve a realistic description of the experiment we must incorporate from the very beginning the influence of the environment degrees of freedom on the system dynamics. During the phase 1 of the experiment the cavity interacts with a single Rydberg atom. The natural frequency of the cavity, as previously mentioned, is finely tuned so that it is nearly equal to the Bohr frequency of the atomic transition between the two adjacent circular levels. Because the radiative lifetime of the circular Rydberg atom is much longer than the interaction time of the atom with the cavity, we can describe the atom as a two level system and neglect the spontaneous decay toward the lower levels [8].

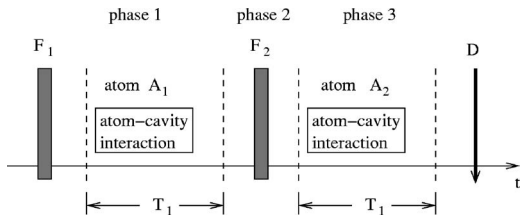

FIG. 2. Timing of the experiment.

Under these conditions the Hamiltonian of the atom-cavity system coincides, within the "rotating wave approximation," with the well-known JC model [9]

$$H_{\mathrm{AF}} = \hbar\omega_a S_z + \hbar\omega_c a^\dagger a + \hbar\Omega(a^\dagger S_- + aS_+), \tag{1}$$

where Ω is the "vacuum Rabi frequency" and $\omega_a(\omega_c)$ is the atomic transition (resonator) frequency. The operators S_+, S_-, S_z are the usual atomic operators for a two-level atom whereas a and $a^\dagger$ are the annihilation and creation operators of the cavity mode.

We will take into account the dissipative effect of the cavity adopting the Markovian quantum master equation which describes the coupling of the cavity system with a bath at zero temperature.

Summing up during the phase 1 the evolution of the system may be described in term of the following master equation [10]:

$$\frac{d}{dt}\rho = -\frac{i}{\hbar}[H_{\mathrm{AF}}, \rho] + \mathcal{L}_F\rho \tag{2}$$

where the superoperator $\mathcal{L}_F$ is defined as

$$\mathcal{L}_F\rho = -\frac{\kappa}{2}(a^\dagger a\rho + \rho a^\dagger a - 2a\rho a^\dagger), \tag{3}$$

κ being the reciprocal of the decay time of the photons inside the cavity.

During the phase 2 there are no atoms inside the cavity and a coherent field, produced by the microwave source S, is injected into C. We can describe this microwave signal, having amplitude $\mathcal{E}$ and angular frequency ω, as a classical one which forces the mode of the cavity. This situation may be represented by means of the following Hamiltonian not involving any atomic degrees of freedom:

$$H_2 = \hbar\omega_c a^\dagger a + (\mathcal{E}e^{-i\omega t}a^\dagger + \mathcal{E}^* e^{i\omega t}a). \tag{4}$$

Also in this phase the cavity cannot be considered as isolated so that its dynamics is described by the following master equation:

$$\frac{d}{dt}\rho = -\frac{i}{\hbar}[H_2, \rho] + \mathcal{L}_F\rho. \tag{5}$$

Concerning the last phase 3 we may repeat the analogous description previously used for the phase 1, namely Eq. (2), provided that the atomic degrees of freedom are now referred to atom A_2.

III. SOLUTIONS OF THE MASTER EQUATIONS

A. Phase 1

To solve the master equation (2) it is convenient to expand ρ into the basis of the dressed states of the atom-cavity system,

$$|\gamma_n^+\rangle = \cos\theta_n|n+1,g\rangle + \sin\theta_n|n,e\rangle,$$
$$|\gamma_n^-\rangle = -\sin\theta_n|n+1,g\rangle + \cos\theta_n|n,e\rangle, \tag{6}$$

where θ_n is given by

$$\tan 2\theta_n = \frac{2\Omega_n}{\delta} \tag{7}$$

with

$$\Omega_n = \Omega\sqrt{n+1} \tag{8}$$

and $\delta=\omega_c-\omega_a$.

Let us now consider the matrix element of the density operator ρ,

$$\rho_{n\nu}^{\epsilon\mu} \equiv \langle\gamma_n^\epsilon|\rho|\gamma_{n+\nu}^\mu\rangle \tag{9}$$

with ϵ, $\mu=\pm$ and $n,\nu\in\mathbb{N}$. If we fix the values of n and ν we can dispose these matrix elements in a four-component vector,

$$\rho_{n\nu} = \begin{pmatrix} \rho_{n\nu}^{++} \\ \rho_{n\nu}^{+-} \\ \rho_{n\nu}^{-+} \\ \rho_{n\nu}^{--} \end{pmatrix}. \tag{10}$$

As a consequence we can write Eq. (2) in the form

$$\frac{d}{dt}\rho_{n\nu} = L_{n\nu}\rho_{n\nu} + \Gamma_{n\nu}\rho_{n+1,\nu}, \tag{11}$$

where $L_{n\nu}$ and $\Gamma_{n\nu}$ are, for each value of n and ν, 4×4 matrices given by

$$L_{n\nu} = -i\nu\omega\,\mathbb{I} - i\begin{pmatrix} \Omega'_n-\Omega'_{n+\nu} & 0 & 0 & 0 \\ 0 & \Omega'_n+\Omega'_{n+\nu} & 0 & 0 \\ 0 & 0 & -\Omega'_n-\Omega'_{n+\nu} & 0 \\ 0 & 0 & 0 & -\Omega'_n+\Omega'_{n+\nu} \end{pmatrix} - \frac{\kappa}{2}\begin{pmatrix} n+c_n^2 & 0 & -s_nc_n & 0 \\ 0 & n+c_n^2 & 0 & -s_nc_n \\ -s_nc_n & 0 & n+s_n^2 & 0 \\ 0 & -s_nc_n & 0 & n+s_n^2 \end{pmatrix}$$
$$-\frac{\kappa}{2}\begin{pmatrix} L_c & -s_{n+\nu}c_{n+\nu} & 0 & 0 \\ -s_{n+\nu}c_{n+\nu} & L_s & 0 & 0 \\ 0 & 0 & L_c & -s_{n+\nu}c_{n+\nu} \\ 0 & 0 & -s_{n+\nu}c_{n+\nu} & L_s \end{pmatrix} \tag{12}$$

with

$$c_n = \cos\theta_n,$$
$$s_n = \sin\theta_n,$$
$$L_c = n+\nu+c_{n+\nu}^2, \tag{13}$$
$$L_s = n+\nu+s_{n+\nu}^2,$$
$$\Omega'_n = \sqrt{\Omega_n^2+\delta^2/4},$$

and

$$\Gamma_{n\nu} = \kappa\begin{pmatrix} \alpha_n^+\alpha_{n+\nu}^+ & \alpha_n^+\alpha_{n+\nu}^- & \alpha_n^-\alpha_{n+\nu}^+ & \alpha_n^-\alpha_{n+\nu}^- \\ \alpha_n^+\beta_{n+\nu}^+ & \alpha_n^+\beta_{n+\nu}^- & \alpha_n^-\beta_{n+\nu}^+ & \alpha_n^-\beta_{n+\nu}^- \\ \beta_n^+\alpha_{n+\nu}^+ & \beta_n^+\alpha_{n+\nu}^- & \beta_n^-\alpha_{n+\nu}^+ & \beta_n^-\alpha_{n+\nu}^- \\ \beta_n^+\beta_{n+\nu}^+ & \beta_n^+\beta_{n+\nu}^- & \beta_n^-\beta_{n+\nu}^+ & \beta_n^-\beta_{n+\nu}^- \end{pmatrix}, \tag{14}$$

where

$$\alpha_n^+ = \sqrt{n+2}c_{n+1}c_n + \sqrt{n+1}s_{n+1}s_n,$$
$$\beta_n^+ = -\sqrt{n+2}c_{n+1}s_n + \sqrt{n+1}s_{n+1}c_n,$$
$$\alpha_n^- = -\sqrt{n+2}s_{n+1}c_n + \sqrt{n+1}c_{n+1}s_n, \tag{15}$$
$$\beta_n^- = \sqrt{n+2}s_{n+1}s_n + \sqrt{n+1}s_{n+1}s_n.$$

In order to obtain an analytical solution of Eq. (11) it is necessary to make some approximations. If we examine the expression of $L_{n\nu}$ we note that whenever $n\gg1$ the matrix can be considered approximatively diagonal. For $\Gamma_{n\nu}$ we note instead that, if the detuning is sufficiently small so that the relation $\delta\ll\Omega\sqrt{n+1}$ holds, we have $s_n\simeq c_n\simeq1/\sqrt{2}$ so that $\Gamma_{n\nu}$ can be approximated by a diagonal matrix as well.

Thus if the detuning δ is small enough and $n\gg1$ we can decouple the matrix equation (11) in four separate equations of the form

$$\frac{d}{dt}\rho_{n\nu}^{\epsilon\mu} = a_{n\nu}^{\epsilon\mu}\rho_{n\nu}^{\epsilon\mu} + b_{n\nu}^{\epsilon\mu}\rho_{n+1,\nu}^{\epsilon\mu}, \tag{16}$$

where the coefficients $a_{n\nu}^{\epsilon\mu}$ and $b_{n\nu}^{\epsilon\mu}$ can be deduced, respectively, from $L_{n\nu}$ and $\Gamma_{n\nu}$. Equation (16) is a tridiagonal linear equation that can be easily treated by using an eigenvalues approach as illustrated in Appendix A. It is important, however, to underline that the equation obtained in corrispondence of $\nu=0$ should be treated separately by taking the sum and the difference of $\rho_{n,0}^{++}$ and $\rho_{n,0}^{--}$.

B. Phase 2

The system described by the master equation (5) is a damped quantum harmonic oscillator forced by a sinusoidal signal with angular frequency ω. In the experiment the frequency of the driving force is tuned with the natural frequency ω_c of the cavity but in our analysis it is convenient not to make *a priori* any particular assumption about ω in order to evidence possible detuning effects.

A well-known result in classical mechanics says that the dynamics of a forced harmonic oscillator can be easily traced back to that of a free harmonic oscillator. We will show that in the case of a sinusoidal driving force this property holds for a quantum harmonic oscillator too.

To this end we consider the following time-dependent transformation of the density matrix of the system:

$$\tilde{\rho}(t) = D(\gamma)T(\omega t)\rho(t)T^{\dagger}(\omega t)D^{\dagger}(\gamma), \tag{17}$$

where

$$D(\gamma) \equiv e^{\gamma a^{\dagger} - \gamma^{*} a} \tag{18}$$

is the Glauber displacement operator with $\gamma \in \mathbb{C}$ and

$$T(\lambda) = \exp(i\lambda a^{\dagger}a) \tag{19}$$

is the unitary operator transforming a into $a\exp(i\lambda)$.

Choosing

$$\gamma = i\frac{\mathcal{E}/\hbar}{i(\omega-\Omega)+\kappa/2} \tag{20}$$

the master equation (5) in terms of the transformed density matrix $\tilde{\rho}(t)$ becomes

$$\frac{d}{dt}\tilde{\rho} = -i\omega'[a^{\dagger}a,\tilde{\rho}] + \mathcal{L}_F\tilde{\rho}, \tag{21}$$

where $\omega' = \omega_c - \omega$. We can note that this latter equation coincides with that of a quantum free damped oscillator. Equation (21), in turn, can be exactly solved with the method illustrated in Appendix B.

Now we will introduce some further considerations about the transformation given by Eq. (17). To this purpose it is convenient to introduce the following superoperators:

$$\mathcal{T}P = [a^{\dagger}a, P], \tag{22}$$

$$\mathcal{D}(\gamma)P = [-i\gamma a^{\dagger} + i\gamma^{*}a, P], \tag{23}$$

where P is an arbitrary operator acting on the oscillator Hilbert space. With the help of these superoperators the transformation (17) can be cast in the form

$$\tilde{\rho}(t) = e^{i\mathcal{D}(\gamma)}e^{i\mathcal{T}\omega t}\rho(t). \tag{24}$$

Using definitions (22) and (23) we can write a formal integral of Eq. (21),

$$\tilde{\rho}(t') = e^{(-i\omega'\mathcal{T}+\mathcal{L}_F)(t'-t)}\tilde{\rho}(t) = e^{-i\omega'\mathcal{T}(t'-t)}e^{-i\omega'\mathcal{L}_F(t'-t)}\tilde{\rho}(t), \tag{25}$$

where the property $[\mathcal{T},\mathcal{L}_F]=0$ has been used.

Transforming back from $\tilde{\rho}$ to ρ, the complete evolution during phase 2 assumes the following form:

$$\rho(t) = e^{-i\mathcal{T}\omega t}e^{-i\mathcal{D}(\gamma)}e^{-i\mathcal{T}\omega' t}e^{\mathcal{L}_F t}e^{i\mathcal{D}(\gamma)}\rho(0), \tag{26}$$

where we have assumed $t=0$ as the beginning time of phase 2.

This expression simplifies even more if we suppose that the force has the same frequency of the cavity. Putting indeed $\omega_c=\omega$ we have

$$\rho(t) = e^{-i\mathcal{T}\omega t}e^{-i\mathcal{D}(\gamma)}e^{\mathcal{L}_F t}e^{i\mathcal{D}(\gamma)}\rho(0). \tag{27}$$

Now we will show that we can further simplify the last expression obtained for the time evolution during phase 2.

Let us start by considering the relation of commutation between $\mathcal{D}(\gamma)$ and $\mathcal{L}_F$. We have

$$[\mathcal{D}(\gamma),\mathcal{L}_F] = -\frac{\kappa}{2}\mathcal{D}(\gamma); \tag{28}$$

by doing some nontrivial algebra we obtain the exact following relation:

$$e^{i\mathcal{D}(\gamma)}e^{\mathcal{L}_F t}e^{-i\mathcal{D}(\gamma)} = e^{i(1-e^{-\kappa t/2})\mathcal{D}(\gamma)}e^{\mathcal{L}_F t}. \tag{29}$$

Equation (29) is particularly useful in the case where the force is very intense and acts for a very small time. In fact if we suppose that

$$|\mathcal{E}| \to \infty, \quad t \to 0, \quad \text{and } \mathcal{E}t/\hbar \to \chi \tag{30}$$

we obtain

$$\begin{aligned} e^{\mathcal{L}_F t} &\simeq 1, \\ e^{i(1-e^{-\kappa t/2})\mathcal{D}(\gamma)} &\simeq e^{i\kappa t/2\mathcal{D}(\gamma)} = e^{i\mathcal{D}(i\chi)}. \end{aligned} \tag{31}$$

This latter equation says that the net effect of an intense resonant driving field for a short time is equivalent to a small displacement of the state of the system into its phase space without any decoherence effect.

We can conclude by saying that the dynamics of the system during phase 2 is given at resonance by expression (27) where the action of $\exp(\mathcal{L}_F t)$ on a generic density matrix ρ can be conveniently evaluated by using expression (B8) with $\omega_0=0$. On the other hand, the action of the displacement operator is evaluated in the number state basis by means of the following relation:

$$\langle n|e^{i\mathcal{D}(\gamma)}\rho|m\rangle = \langle n|D(\gamma)\rho D^{\dagger}(\gamma)|m\rangle$$
$$= \sum_{i=0}^{\infty} \langle n|D(\gamma)|i\rangle\langle i|\rho|j\rangle\langle j|D(\gamma)|m\rangle, \quad (32)$$

where the matrix elements of the displacement operator are given by [11]

$$\langle m|D(\xi)|n\rangle = \sqrt{\frac{n!}{m!}}\xi^{m-n}e^{-|\xi|^2/2}L_n^{(m-n)}(|\xi|^2) \quad (33)$$

with $L_n^{(\alpha)}$ being the generalized Laguerre polynomial.

We can also make use of Eq. (29) to confine ourselves to low excitations number when very intense driving fields acting for a short period of time are in order.

IV. DISCUSSION OF THE PROBING PROCEDURE

In the last section we have developed the mathematical tools which allow as to solve analytically the temporal evolution of the system in the different phases. Now we want to discuss from the physical point of view phases 2 and 3 of the experiment. Equations (26) and (27) reported in Sec. III B enable us to claim that, generally speaking, the effect of the driving signal during phase 2 is twofold. On the one hand it does cause a translation of the cavity state in its phase space due to the presence of superoperators of the form $\exp D(\gamma)$. On the other hand the presence of a superoperator like $\exp(\mathcal{L}_F t)$ is at the origin of dissipation and decoherence effects.

To understand the physical mechanism by which the second atom detects the state of the cavity after phase 2 let us analyze a simple case ignoring for the moment the presence of the cavity losses. If the cavity is in a coherent state $|\alpha\rangle$ with $\alpha \gg 1$ the atom is subjected to Rabi oscillations with an angular frequency of about $\Omega|\alpha|$. These oscillations then get damped after a time of the order of $1/\Omega$ and the probability to find the atom in its ground state settles down to the value of $1/2$. On the other hand, for $\alpha \ll 1$ the cavity is approximately in its vacuum state and, because the atom is prepared in its ground state, the system does *not* perform any oscillation. Thus when $\alpha \ll 1$ the probability of finding the atom in the ground state is roughly 1.

If after phase 1 the system were in a coherent state $|\alpha\rangle$ then the net effect of the driving field would be a translation,

$$\alpha \to \alpha + \Delta e^{i\phi}, \quad (34)$$

with Δ being a complex parameter depending on the amplitude and the duration of the signal. If amplitude and duration are appropriately calibrated then Eq. (34) says that a particular value ϕ_0 of the phase ϕ will bring the cavity into its vacuum state. In this case $S_g(\phi)$ assumes a value near to the unity. Other values of ϕ would lead to coherent state $|\alpha'\rangle$ with $\alpha' \gg 1$. As a consequence the atom would be subjected to the Rabi oscillations which will subsequently get damped so that the probability $S_g(\phi)$ would assume the value of $1/2$.

Summing up, if the cavity is in a coherent state after phase 1 then the probing performed in phases 2 and 3 with the help of the atom A_2 will produce a pattern of $S_g(\phi)$ characterized by a maximum for a particular value ϕ_0 of ϕ and a constant value of 0.5 elsewhere. This situation is qualitatively illustrated in Fig. 3.

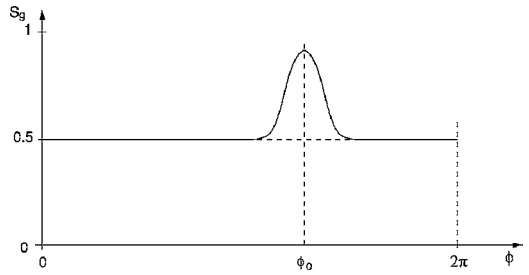

FIG. 3. Qualitative behavior of $S_g(\phi)$ when the cavity is left in a coherent state $|\alpha\rangle$ after phase 1.

If the state of the cavity after the injection of the microwave signal F_2 is $|\alpha\rangle$ then S_g will be given by the following expression:

$$S_g(\alpha) = \frac{1}{2} - \langle S_z\rangle = e^{-|\alpha|^2}\sum_{n=0}^{\infty}\frac{|\alpha|^{2n}}{n!}\cos^2(\Omega\sqrt{n}t). \quad (35)$$

In Fig. 4 we have reported a plot of S_g in function of $|\alpha|$ for different values of Ωt.

We can see that when $\alpha=0$, $S_g=1$, and, for $\alpha\to\infty$, the value of S_g settles down around the value of $1/2$ with the exception of the graph for $\Omega t=\pi/2$. This exception happens because the time t is short and the Rabi oscillations does not have the time to completely disappear. In fact we know that the Rabi oscillations disappears in a time of the order of $1/\Omega$ independently from α. So we can say that for *small* values of t we have an oscillating behavior of $S_g(\alpha)$. We also note from Fig. 4 that for particular values of the interaction time and α we obtain a probability to find the atom in its ground state $S_g < 1/2$. This in turn implies that the curve of $S_g(\phi)$, Fig. 3, can have also some secondary minima besides of the main peak.

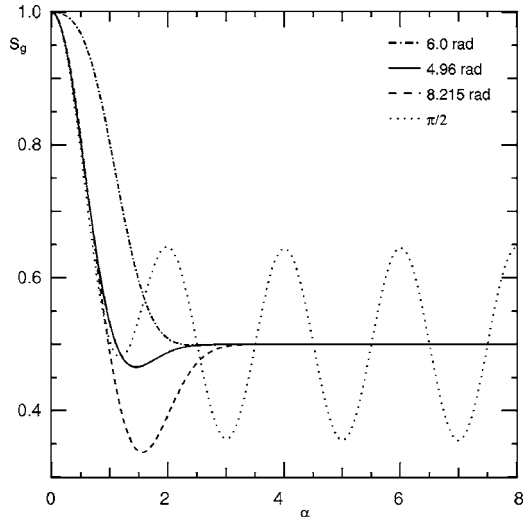

FIG. 4. S_g against $|\alpha|$ for different values of Ωt.

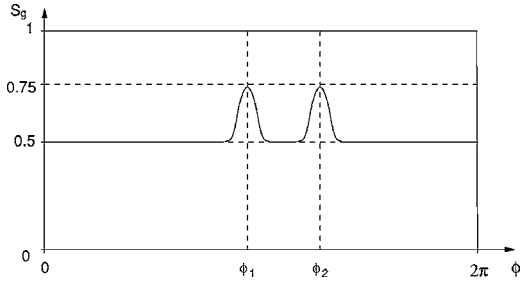

FIG. 5. Qualitative behavior of $S_g(\phi)$ when the system is left in a superposition of two coherent states at the beginning of phase 2.

In the experiment [7] the actual interaction time between the atom and the cavity gives for Ωt the values 4.96 rad and 8.215 rad. Observing Fig. 4 we note that the plots for $\Omega t = 4.96$, 8.215 rad does not have an oscillatory behavior but they have a minimum value below 1/2 before approaching the asymptotic limit.

Suppose now that the intensity and the duration of the driving field F_2 is such that after phase 2 the cavity is left in the state

$$|\psi_1\rangle = c(|0\rangle + |\beta\rangle), \tag{36}$$

c being a normalization constant and where $|\beta\rangle$ is a coherent state with $|\beta| \gg 1$. During phase 3 the state $|\psi_1\rangle$ of the cavity is probed by the atom A_2.

As a consequence of the interaction of A_2 and the cavity the quantity S_g is the sum of three terms,

$$S_g = |c|^2\left(\frac{1}{2} + 1\right) + (\text{interference terms}), \tag{37}$$

one of which is directly related to the interference between the two coherent components of $|\psi_1\rangle$. In the limit $|\beta| \gg 1$ this interference term can be neglected being $\langle 0|\beta\rangle \simeq 0$ and in addition $c^2 \simeq \frac{1}{2}$. Thus $S_g \simeq 0.75$ when $|\beta| \gg 1$. If on the other hand the state of the cavity is

$$|\psi_2\rangle = c'(|\alpha'\rangle + |\beta'\rangle) \tag{38}$$

with both $|\alpha'| \gg 1$ and $|\beta'| \gg 1$ the correspondent value of S_g after phase 3 will be $\simeq 0.5$. We thus may claim that there exist two appropriate values of the phase ϕ of F_2 such that $S_g(\phi)$ presents two maxima when after phase 1 the cavity is left in a superposition of two coherent states like that expressed by Eq. (38). Such a qualitative behavior of $S_g(\phi)$ is reported in Fig. 5.

V. RESULTS AND DISCUSSION OF THE EXPERIMENT

To start with phase 1, the cavity is prepared in a coherent state so that its density matrix is given by

$$\rho_F(0) = e^{-|\alpha|^2}\sum_{n=0}^{\infty}\sum_{m=0}^{\infty}\frac{\alpha^n \alpha^{*m}}{\sqrt{n\,!\,m!}}|n\rangle\langle m|. \tag{39}$$

If we suppose that the atom A_1 is initially prepared in its upper circular Rydberg state, the density matrix of atom-cavity system at the beginning of phase 1 may be represented as

$$\rho(0) = \rho_F(0) \otimes |e\rangle\langle e|. \tag{40}$$

The evolution of the system during this phase is investigated with the help of Eq. (11). In the experiment described in Ref. [7] two different values for the interaction time T_1 between the atom and the cavity, i.e., $T_1 = 32$ μs and $T_1 = 53$ μs, were chosen.

Since no measurement is performed on atom A_1, the initial state of the cavity in phase 2, that is, just before injecting the signal F_2, may be obtained tracing the atom A_1-cavity density matrix, at the end of phase 1, with respect to the atomic degrees of freedom.

During phase 2 the cavity is driven by a microwave field F_2 whose phase and strength are described by the complex amplitude $\mathcal{E}$. In accordance with Ref. [7] such a driving field acts upon the cavity for a time $T_2 = 23$ μs. Three physical parameters characterize this part of the experiment, namely the strength $|\mathcal{E}|$ and the phase ϕ of the driving field as well as the duration T_2 of the injected signal.

The impulse F_2 injected into the cavity has the same amplitude of F_1 which determines the initial coherent state created inside the cavity. The evolution of the cavity when subjected to a driving external field is given by Eq. (27). Since we are at resonance, in view of Eq. (20) the parameter γ has the following expression:

$$\gamma = i\frac{\mathcal{E}/\hbar}{\kappa/2}. \tag{41}$$

By looking at Eq. (29) we moreover infer that the displacement of the Wigner function induced by the same driving field is

$$\chi = (1 - e^{-\kappa t/2})\gamma. \tag{42}$$

Hence we conclude that, if the cavity starts in its vacuum state before the injection of F_1, we obtain a coherent state of complex amplitude,

$$\alpha = i\frac{\mathcal{E}/\hbar}{\kappa/2}(1 - e^{-\kappa t/2}). \tag{43}$$

Of course, taking into account that $\kappa^{-1} = 850$ μs [7], the knowledge of the initial coherent state allows us to trace back to the amplitude of both F_1 and F_2. We have succeeded in exactly solving the sequence of all the equations of motion directly related to the experiment reported in Ref. [7] incorporating cavity damping effects. The mathematical expression of $\rho(t)$ after phase 3, that is, when the probing atom A_2 exits the cavity, it is not reported here because it is too involved to be of help in proceeding with the comparison between our analysis and the experimental results. Instead we concentrate on the observed quantity $S_g(\phi)$ which may be evaluated in correspondence to the particular experimental situation considered in Ref. [7].

In Fig. 6 we plot the probability $S_g(\phi)$ of finding the atom A_2 in its ground state in correspondence to atom-cavity interaction time $T_1 = 32$ μs. The atom A_1 is initially prepared in the excited state and the cavity is exactly at resonance with $\bar{n} = 18$. $S_g(\phi)$ shows two maxima in correspondence to the particular values of the phases possessed by the two coherent

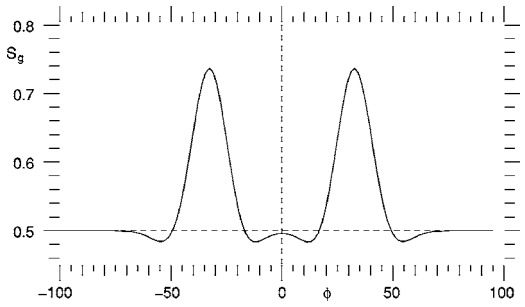

FIG. 6. Predicted curve for $S_g(\phi)$ against ϕ with $\delta=0$ when the atom A_1 is initially prepared in its excited state.

components of the cavity field after interaction with atom A_1. The plot shows some secondary maxima and minima in agreement with the previous discussion.

In Fig. 7 the same quantity $S_g(\phi)$ is reported in correspondence with an off-resonance term comparable with the vacuum Rabi frequency of the system.

We are now ready to compare our theoretical analysis with the experimental results reported in Ref. [7]. We can see that the distance between the two peaks of Fig. 6 is the same of the experimental data as deducible from Fig. 2 of Ref. [7]. We also note that taking into account the presence of detuning $\omega_c-\omega_a=\delta\neq 0$ leads in Fig. 7 to an asymmetrization and an enlargement of the two peaks. This is qualitatively in agreement with the experimental results reported in Ref. [7] where the asymmetry of the two peaks is quite evident. It is in addition clear that the width of the peaks obtained by the experimental data are greater than the width predicted for the ideal case $\delta=0$ and shown in Fig. 6. We draw the conclusion that in the experiment reported in Ref. [7] there might be an off-resonance between the cavity and the atomic transition of the order of magnitude of the vacuum Rabi frequency.

For the sake of a full comparison between our analysis and experimental results of Ref. [7] we wish to conclude this section plotting in Fig. 8 $S_g(\phi)$ when the atom A_1 is initially prepared in its "dipole state":

$$|\phi_a^+\rangle=\frac{1}{\sqrt{2}}(|e\rangle+|g\rangle). \tag{44}$$

It is worth noting that, keeping the values of all the other experimental conditions of Fig. 6, in this case $S_g(\phi)$ is

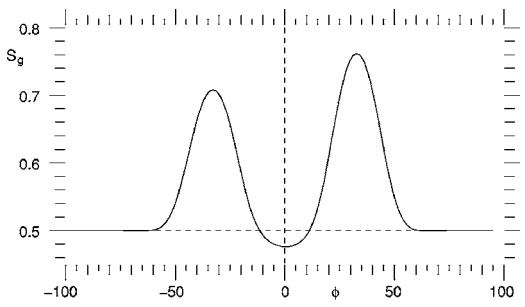

FIG. 7. Predicted curve for $S_g(\phi)$ against ϕ with $\delta/\Omega=1.0$ when the atom A_1 is initially prepared in its excited state.

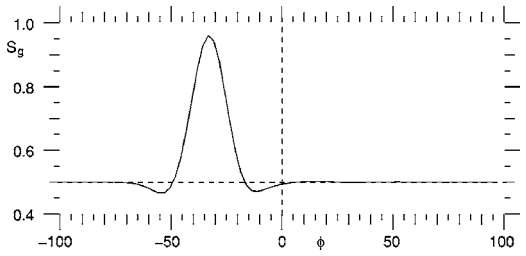

FIG. 8. Predicted curve for S_g in function of ϕ when the atom A_1 is initially in a dipole state.

peaked around a single value of ϕ only in accordance with Fig. 3 of Ref. [7].

VI. CONCLUSIONS

The theoretical investigation presented in this paper has been spurred by a recent experiment aimed at producing and observing the phase entanglement between a mesoscopic cavity field and the atomic dipole of a single Rydberg atom. Our analysis of both the preparation phase of the entangled state and its probing is based on an approach incorporating, from the very beginning, effects stemming from cavity losses. Our treatment, in accordance with the experiment, makes explicitly use of the not too low mesoscopic intensity of the initial coherent field injected into the cavity. This circumstance enables us to analytically solve the dynamical evolution of the system leading to the generation of the entangled state. The probing phase is followed in detail once again taking into due account the cavity losses by considering the appropriate master equation predicting the temporal evolution of the field.

The results of our theoretical investigation are in good qualitative and quantitative agreement with those achieved in laboratory. We have in particular succeeded in establishing a link between experimental found, but not commented, asymmetry of the two peaks exhibited by $S_g(\phi)$ and a slight detuning between atomic and mode natural frequency.

In addition, to suppose the existence of such a small detuning modifies the widths of the two peaks improving in this way, as a matter of fact, the quantitative agreement between our results and the experimental ones.

Another aspect of our treatment is the prediction of secondary minima and maxima in the ϕ dependence of $S_g(\phi)$, which appear even when no detuning is invoked, that is at exact resonance.

It is worth noting that the numerical estimation of our results have been based, when available, on values of the parameters extracted from Ref. [7]. In conclusion we feel that the good degree of agreement between our analysis and the experimental results enforces and further validates a theoretical approach based on fundamental atom-cavity interaction model and simple mathematical structure of dissipative superoperators.

APPENDIX A: SOLUTION OF A CLASS OF TRIDIAGONAL LINEAR EQUATIONS

In this appendix we will illustrate the solution of a particular class of tridiagonal linear differential equations. Let

us consider a set of N variable p_n with $n=1,2,\ldots,N$ whose time dynamics is described by equations of the form

$$\frac{d}{dt}p_n = \alpha_n p_n + \beta_n p_{n+1}, \tag{A1}$$

where α_n and β_n are given coefficients. If we now dispose the terms p_n in a column vector P we can write the differential equations in matrix form

$$\frac{d}{dt}P = M \cdot P, \tag{A2}$$

where M is a $N\times N$ matrix given by

$$M = \begin{pmatrix} \alpha_1 & \beta_1 & 0 & \ldots & 0 \\ 0 & \alpha_2 & \beta_2 & \ldots & 0 \\ \ldots & & & & \ldots \\ 0 & 0 & 0 & \ldots & \alpha_N \end{pmatrix}. \tag{A3}$$

To the purpose of integrating the differential equation (A2) it is useful to diagonalize the matrix M. In fact we can write

$$M = S^{-1}M_\lambda S, \tag{A4}$$

where M_λ is the eigenvalues' matrix

$$M_\lambda = \begin{pmatrix} \alpha_1 & 0 & 0 & \ldots & 0 \\ 0 & \alpha_2 & 0 & \ldots & 0 \\ \ldots & & & & \ldots \\ 0 & 0 & 0 & \ldots & \alpha_N \end{pmatrix}. \tag{A5}$$

The explicit components of matrices S and S^{-1} are given by the following expressions:

$$S_{nk} = \prod_{j=n+1}^{k} \frac{\beta_{j-1}}{\alpha_n - \alpha_j},$$

$$(S^{-1})_{nk} = \prod_{j=n}^{k-1} \frac{\beta_j}{\alpha_k - \alpha_j}. \tag{A6}$$

Once we have diagonalized the matrix M we can immediatly integrate Eq. (A2). We have

$$P(t) = e^{Mt}P(0) = e^{S^{-1}M_\lambda St}P(0) = S^{-1}e^{M_\lambda t}SP(0), \tag{A7}$$

where the matrix $\exp(M_\lambda t)$ can be trivially calculated.

Equation (A7) enable us to solve, either analytically or numerically, every equation of the form (A1).

APPENDIX B: TIME EVOLUTION OF A DAMPED HARMONIC OSCILLATOR

Let us consider a damped harmonic oscillator whose dynamics is described by the equation

$$\frac{d}{dt}\rho = -i\omega_0[a^\dagger a,\rho] + \mathcal{L}\rho, \tag{B1}$$

where $\mathcal{L}$ is the superoperator which describes the dissipative effect, defined by the relation

$$\mathcal{L}P = -\frac{\kappa}{2}(a^\dagger aP + Pa^\dagger a - 2aPa^\dagger). \tag{B2}$$

To obtain a solution of Eq. (B1) we take the matrix element of both sides in the Fock number states basis getting

$$\frac{d}{dt}\rho_{nm} = -i\omega(n-m)\rho_{nm} - \frac{\kappa}{2}[(n+m)\rho_{nm} - 2\sqrt{(n+1)(m+1)}\rho_{n+1,m+1}]. \tag{B3}$$

If we now replace the index m with $n+\nu$, where ν is an integer, we note that the equations only couple terms with the same ν and different value of n. So for each value of ν we have a chain of differential equations of the form (A1).

Then we can solve Eq. (B3) by using the method illustrated in Appendix A. In fact the coefficients α_n and β_n for Eq. (B3) (for each value of ν) are given by

$$\begin{cases} \alpha_n = i\omega\nu - \dfrac{\kappa}{2}(2n+\nu), \\ \beta_n = \kappa\sqrt{n+1}\sqrt{n+\nu+1}. \end{cases} \tag{B4}$$

From the explicit expressions of coefficients α_n and β_n we obtain for the matrix S the following expression:

$$S_{nk} = \sqrt{\binom{k}{n}\binom{k+\nu}{n+\nu}} \tag{B5}$$

and for the inverse matrix

$$(S^{-1})_{nk} = (-1)^{k-n}\sqrt{\binom{k}{n}\binom{k+\nu}{n+\nu}}. \tag{B6}$$

Then by using Eq. (A7) we obtain for the coefficient $p_n(t)$ of Eq. (A1) the following expression:

$$p_n(t) = e^{i\omega\nu t - \kappa\nu t/2}\sum_{j=n}^{\infty}\sqrt{\binom{j}{n}\binom{j+\nu}{n+\nu}}e^{-\kappa nt}(1-e^{-\kappa t})^{j-n}p_j(0). \tag{B7}$$

Exchanging $p_n(t)$ with $\rho_{n,n+\nu}(t)$ in Eq. (B7) yields the following explicit solution for Eq. (B3):

$$\rho_{n,n+\nu}(t) = e^{i\omega\nu t}e^{-\kappa(n+\nu/2)t}, \sum_{m=n}^{\infty}\rho_{m,m+\nu}(0)\sqrt{\binom{m}{n}\binom{m+\nu}{n+\nu}}(1-e^{-\kappa t})^{m-n}. \tag{B8}$$

Equation (B8) gives the state of the system at time t for any initial state $\rho(0)$.

Incidentally we note that, if we pose $\omega=0$, we can consider the expression obtained as a means to evaluate the operator $\exp(\mathcal{L}_F t)$. In fact, Eq. (B8) (with $\omega=0$) gives the solution of the equation

$$\frac{d}{dt}\rho = \mathcal{L}_F\rho$$

for any given initial condition $\rho(0)$. Thus Eq. (B8) gives an explicit expression for the evaluation of operator $\exp(\mathcal{L}_F t)$.

Now let us consider an initial density operator of the form

$$\rho(0) = P(0) = |\alpha\rangle\langle\beta| \tag{B9}$$

whose Fock basis matrix elements are

$$P_{n,n+\nu}(0) = \frac{\alpha^n \beta^{*(n+\nu)}}{\sqrt{n\,!\,(n+\nu)!}} \exp[-|\alpha|^2/2 - |\beta|^2/2] \tag{B10}$$

if $|\alpha\rangle$ and $|\beta\rangle$ are coherent states. Using Eq. (B8) after some algebra we get

$$P_{n,n+\nu}(t) = e^{i\omega\nu t} e^{-\kappa(n+\nu/2)t} \frac{\alpha^n \beta^{*(n+\nu)}}{\sqrt{n\,!\,(n+\nu)!}} \exp[-|\alpha|^2/2 - |\beta|^2/2 + \alpha\beta^*(1-e^{-\kappa t})]. \tag{B11}$$

The density matrix $P(t)$ can be thus expressed as follows:

$$P(t) = |\alpha e^{-i\omega t - \kappa t/2}\rangle\langle\beta e^{-i\omega t - \kappa t/2}| \times \exp\left[\left(-\frac{1}{2}|\alpha-\beta|^2 + i\phi(\alpha,\beta)\right)(1-e^{-\kappa t})\right]. \tag{B12}$$

Equation (B12) is the main element which enables us to write the evolution of an arbitary initial state in the coherent basis. In fact if we develop the initial state $\rho(0)$ using the completeness of the coherent states basis

$$\rho(0) = \frac{1}{\pi^2}\int d^2\alpha \int d^2\beta\; W(\alpha,\beta)|\alpha\rangle\langle\beta| \tag{B13}$$

we can write the state of the system at time t in the form

$$\rho(t) = \frac{1}{\pi^2}\int d^2\alpha \int d^2\beta\; W(\alpha,\beta)|\alpha e^{-i\omega t-\kappa t/2}\rangle \times\langle\beta e^{-i\omega t-\kappa t/2}| \cdot \exp\left[\left(-\frac{1}{2}|\alpha-\beta|^2 + i\phi(\alpha,\beta)\right) \times(1-e^{-\kappa t})\right].$$

This latter equation expresses the time evolution of a damped harmonic oscillator described by Eq. (B1) in the coherent basis.

[1] C. J. Myatt *et al.*, Nature (London) **403**, 269 (2000).
[2] C. Monroe, D. M. Meekhof, B. E. King, and D. J. Wineland, Science **272**, 1131 (1996).
[3] A. Ben-Kish *et al.*, Phys. Rev. Lett. **90**, 037902 (2003).
[4] M. Brune *et al.*, Phys. Rev. Lett. **77**, 4887 (1996).
[5] Guang-Sheng Jin *et al.*, Phys. Rev. A **69**, 034302 (2004).
[6] J.-M. Raimond, M. Brune, and S. Haroche, Rev. Mod. Phys. **73**, 565 (2001).
[7] A. Auffeves *et al.*, Phys. Rev. Lett. **91**, 230405 (2003).
[8] S. Haroche, in *Fundamental Systems in Quantum Optics*, edited by J. Dalibard, J. M. Raimond, and J. Zinn-Justin (North-Holland, Amsterdam, 1992), p. 771.
[9] E. T. Jaynes and F. W. Cummings, Proc. IEEE **51**, 89 (1963).
[10] F. Petruccione and H. P. Breuer, *The Theory of Open Quantum System* (Oxford University Press, New York, 2002).
[11] K. E. Cahill and R. J. Glauber, Phys. Rev. **177**, 1857 (1969).